TI 2026-057/III
Tinbergen Institute Discussion Paper

A Dynamic Nonlinear Panel Decomposition Model for the Global Environmental Kuznets Curve

Cheyenne Amoroso[1]
Carolina Garcia-Martos[2]
Siem Jan Koopman[3]

1 Universidade da A Coruna

2 Universidad Politecnica de Madrid

3 Vrije Universiteit Amsterdam and Tinbergen Institute

A Dynamic Nonlinear Panel Decomposition Model for the Global Environmental Kuznets Curve

Cheyenne Amoroso[1], Carolina García-Martos[2], and Siem Jan Koopman[3]

[1]Department of Mathematics, MODES, Universidade da A Coruña, Campus de Elviña, 15071 A Coruña, Spain. cheyenne.amoroso@udc.es
[2]Escuela Técnica Superior de Ingenieros Industriales, Universidad Politécnica de Madrid, C/ José Gutiérrez Abascal 2, 28006 Madrid, Spain. garcia.martos@upm.es
[3]Department of Econometrics, Vrije Universiteit Amsterdam, De Boelelaan 1105, 1081 HV Amsterdam, The Netherlands. s.j.koopman@vu.nl

Abstract

We propose a decomposition of the Environmental Kuznets Curve (EKC) based on a difference-of-sigmoid functions with one for the economic-growth effect and one for the green-economy effect. This nonlinear function replaces the traditional quadratic specification in panel data models. We further extend the framework with unobserved stochastic trends to capture time-varying features such as evolving energy mixes and technological advances. The panel model can be represented in state-space form. We show that parameter estimation can be carried out by nonlinear regression and Kalman filter methods. In our empirical study, we consider a panel of pollution (CO_2 emissions) and economic output variables for 15 major economies (G7, Australia and 7 emerging countries), representing approximately 75% of the global economy. We extract the common EKC where its parameters are pooled or partially pooled across all countries. The empirical results show statistically significant evidence of a global relevant EKC.

Keywords: Environmental Kuznets Curve, nonlinear panel data model, stochastic trends, state-space methods.

1 Introduction

The Intergovernmental Panel on Climate Change, IPCC (2023), has provided strong evidence that human activities drive widespread warming and rising climate risks. These concerns led to international commitments under the United Nations Framework Convention on Climate Change, notably the Kyoto Protocol and the Paris Agreement, UNFCCC (1997, 2015). More recently, climate change has come to be understood not only as an environmental problem but also as a source of economic and financial risk. The evidence for this is substantive. Dell et al. (2012) argue that increasing temperature levels affect development trajectories and long-run welfare. Bolton and Kacperczyk (2021) find that carbon exposure is priced in financial markets, with investors requiring compensation for carbon risk. This motivates the use of econometric models linking growth, emissions and transition dynamics.

The Kuznets curve originates in Kuznets (1955) who studied the relationship between economic development and income inequality. The Environmental Kuznets Curve (EKC) adopts his framework to the trade-off between economic development and environmental degradation, positing an inverted U-shaped relationship: as per-capita GDP rises, per-capita CO_2 emissions first increase and then decline once a critical income threshold is passed. This principle of "grow first, clean later", highlighted by Grossman and Krueger (1991, 1995) and Holtz-Eakin and Selden (1995), has shaped debates on whether economic growth can ultimately become compatible with sustainability. This pattern is driven by a scale effect, or composition effect, as economies shift from heavy industry toward cleaner sectors, and a technological effect, as rising demand for environmental quality leads governments to regulate and to subsidize cleaner technologies. This interpretation of the EKC is questioned in Castle and Hendry (2026), who stress that the use of fossil-fuels, not economic growth, is the causal driver of emissions. In other words, the link between economic activity and emissions evolves over time.

Early EKC research relied on cross-sectional and panel regressions with quadratic specifications of economic output. Shafik and Bandyopadhyay (1992), Panayotou (1993) and Grossman and Krueger (1995) find inverted U-shaped patterns for several pollutants, popularizing the idea that growth might be the solution to pollution rather than its cause. However, Cole et al. (1997) show that the results depend on which pollutant is chosen, while List and Gallet (1999) emphasize cross-country heterogeneity. Therefore, the research shifted toward nonlinear models designed to address endogeneity, omitted variables and cross-sectional dependence.

From the early 2000s, the robustness of these findings was increasingly questioned. Stern (2004) criticize earlier studies for omitted variables, inappropriate functional forms and neglect of non-stationarity. This prompted a move toward the panel cointegration and error-correction models of Perman and Stern (2003) and Apergis and Payne (2009), as well as alternative nonlinear specifications; see Hansen (1999) and Fosten et al. (2012).

Empirical evidence for the EKC nonetheless remains mixed. Leal and Marques (2022) conclude that the evidence is highly sensitive to model specification, variable choice and sample design. Other work points to features that aggregate specifications tend to miss. Maddison (2006) shows that spatial dependence can alter EKC inferences, so that ignoring cross-country spillovers may misrepresent the transition dynamics. Montagna et al. (2025) find that aggregate curves can hide strong sectoral heterogeneity, with turning points and decoupling depending on how individual industries evolve. A more fundamental concern relates to econometrics. Wagner (2015) shows that when economic output x_t is integrated of order one, its powers are generally not integrated of any order, so treating x_t, x_t^2 and x_t^3 as integrated regressors in standard cointegration procedures yields invalid inference and spurious support for an EKC-type relationship. Related work develops problem-adequate methods for cointegrating polynomial regressions; see Wagner et al. (2020) and De Jong and Wagner (2025).

More recent work extends the EKC framework by incorporating broader drivers and heterogeneity across development paths. Wang et al. (2024) find that institutional, technological, resource, and social factors can shape the estimated income-emission relationship, using data for 214 countries over 1960–2020,. Li et al. (2024) bring in geopolitical risk, natural resource rents, governance, and energy intensity. Wang et al. (2024) re-examine the EKC for both carbon emissions and the ecological footprint in a global panel of 147 countries (1995–2018), finding that trade openness acts as a nonlinear threshold-type moderator with heterogeneous effects. Taken together, these studies suggest that globalization and trade regimes shape the growth-environment relationship beyond static polynomial specifications for income or growth. Finally, Bennedsen et al. (2023) propose a neural-network approach to the income-emissions relationship; they demonstrate that the EKC is not a universal structural relationship but a region-specific, data-driven pattern that depends critically on model flexibility and the definition of emissions. Our study aims to address these findings by holding on to a parametric specification for the EKC and accounting for stochastic trends.

We introduce a dynamic statistical model that decomposes the EKC curve into two interpretable components: an early economic-growth effect and a later green-transition effect driven by technological and institutional change. This decomposition preserves the 'grow first, clean later' interpretation while giving each phase an explicit functional form. Polynomial specifications imply unbounded emissions. Our proposed asymmetric difference-of-sigmoids (DoS) function is bounded. It uses logistic components that can capture early-stage growth and the subsequent green transition. Also, the DoS function is immune, by construction, to the integration problem raised by Wagner (2015), since a bounded time series variable cannot be integrated of any order; see Phillips (1987).

To account for non-stationary features in the time series, we add stochastic trends to the dynamic nonlinear panel model with the DoS curve. Stochastic trends accommodate gradual transitions, latent dynamics, time-varying relationships, and omitted variables. The resulting model can be formulated in state-space form and related methods such as the Kalman filter are well suited when the signal is persistent, the measurements noisy, and the underlying relationships are evolving. In econometrics, this approach connects to well-established foundations for time series analysis developed by Koopman et al. (1999) and Durbin and Koopman (2012), and to climate-oriented applications, where the extraction of evolving trends is crucial, as demonstrated by Gao and Hawthorne (2006), Keane and Neal (2020) and Bennedsen et al. (2023). We adopt the method of maximimum likelihood for parameter estimation and the state-space bootstrap method for computing standard errors and confidence intervals.

In our empirical study, we consider a country-panel for the two time series variables CO_2 emissions, as a proxy of pollution, and GDP, as a proxy of economic output, both in logs and per-capita, for 15 major economies (G7, Australia and 7 emerging countries). We extract the DoS function, representing the EKC, with its parameters being pooled across all countries. We also include specifications for only the G7 plus Australia, only the 7 emerging countries, and all countries but with non-pooled parameter for European countries. The empirical results show statistically significant evidence of a global relevant EKC, with Europe adopting an early green transition.

The remainder of the paper is organized as follows. Section 2 presents the dynamic nonlinear panel data model with stochastic trends. Section 3 describes the estimation procedure of the DoS specification and latent trends using state-space methods as well as bootstrap scheme for making inference. Section 4 reports an empirical study to identify a convincing global EKC for a major panel of 15 countries. Finally, Section 5 concludes.

2 Nonlinear panel data model with stochastic trends

2.1 The static specification with fixed effects

The structure of our Environmental Kuznets Curve (EKC) decomposition model can be expressed as a country panel data model with nonlinear regression effects given by

$$y_{it} = \mu_i + \gamma \left[\sigma_1(x_{it}; c_1, s_1) - \sigma_2(x_{it}; c_2, s_2)\right] + \varepsilon_{it}, \tag{2.1}$$

where y_{it} is the release of carbon dioxide gas into the atmosphere (CO_2 emissions per capita) for country i in year t, μ_i is the fixed effect for country i, and γ is a fixed amplitude coefficient. The function $\sigma(x; c, s) \in [0, 1]$ is a bounded function in x of the logistic family, with location c determining the activation of the curve and slope s determining the steepness of the transition from 0 to 1. Furthermore, x_{it} is the gross domestic product (GDP per capita) for country i in year t, and ε_{it} is an independent and identically distributed (IID) noise term, for $i = 1, \ldots, N$ and $t = 1, \ldots, T$, with N as the number of countries present in the panel model and T as the time series length (number of years).

The two nonlinear functions $\sigma_1(\cdot)$ and $\sigma_2(\cdot)$ represent the level of economic output and the green transition effects, respectively. The key notion of the EKC is that at higher levels of economic output, climate costs become more pertinent and there is a societal incentive to initiate a green transition, as represented by $\sigma_2(\cdot)$. The latter is often partly driven by government policies. More specifically, $\sigma_1(\cdot)$ captures the early-stage economic growth effect, while $\sigma_2(\cdot)$ captures the late-stage green transition as emissions rise with prosperity. Economic growth and the green transition exist in parallel, the former increases CO_2 emissions while the latter decreases emissions, hence the two nonlinear functions have opposite signs in the specification.

These functions are activated at different levels of GDP, hence the model includes distinct location coefficients, c_1 and c_2. Typically, we have $c_1 < c_2$, which implies that the first transition (increasing emissions) occurs at lower income levels and the second transition (decreasing emissions) at higher income levels. Similarly, the shapes of the two transitions can also be different, as reflected by the two slope coefficients, s_1 and s_2. To ensure that the logistic curves are monotonically increasing, we strictly set $s_1, s_2 > 0$.

Finally, the two functions $\sigma_1(\cdot)$ and $\sigma_2(\cdot)$ are bounded in both directions, positive and negative. This implies that CO_2 releases saturate at some extreme level, but CO_2 reductions also saturate. Similarly, economic production ranges from zero to some extreme upper level, but not infinity. The total effect is scaled by the coefficient γ and is initially pooled for $\sigma_1(\cdot)$ and $\sigma_2(\cdot)$, given that both y_{it} and x_{it} are measured per capita. We can relax this setting and further consider varying coefficients γ_i for each country i. We consider the logistic function in both cases as given by

$$\sigma_j(x_{it}; c_j, s_j) = \frac{1}{1 + \exp[-s_j(x_{it} - c_j)]}, \tag{2.2}$$

for $j = 1, 2$. Finally, it is assumed that the IID noise term ε_{it} has mean zero and variance σ_ε^2 for all i and t. More appropriate variance and covariance specifications can be considered in future work.

The difference $\sigma_1(\cdot) - \sigma_2(\cdot)$ is defined as the difference-of-sigmoid (DoS) function which is smooth and has an inverted asymmetric U-shape. It is our proposal of a flexible and interpretable representation of the EKC. The locations and shapes of this curve are determined by the values of c_1, c_2, s_1 and s_2, while the amplitude of the EKC is determined by the coefficient γ, which represents the overall effect size. The turning point of the DoS can be determined analytically in some restricted cases and numerically in all other cases. In the Appendix A.1, we prove the existence of a turning point of the DoS, its strict concavity in $c1, c2$, its uniqueness, and its global-maximizer property. These properties hold under the EKC conditions $c_1 < c_2$ and $s_1, s_2 > 0$.

Figure 1 illustrates how the DoS is constructed from two logistic components. Their difference forms the structural EKC trajectory with a unique turning point. The DoS setting is flexible allowing for different shapes, including sharp transitions possibly due to countries leapfrogging specific technologies. The strict parameterization can be relaxed. For example, two coefficients γ_1 and γ_2 for $\sigma_1(\cdot)$ and $\sigma_2(\cdot)$, respectively. This case accommodates countries with net-negative emissions, we then have $\gamma_1 < \gamma_2$.

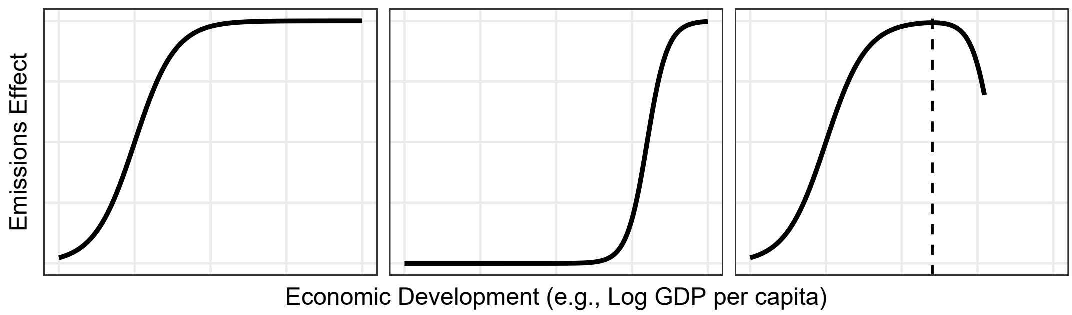

Figure 1: Difference-of-sigmoid (DoS) function: $\sigma_1(\cdot)$ with $c_1 = 2.5, s_1 = 1.5$ (left), $\sigma_2(\cdot)$ with $c_2 = 8, s_2 = 3$ (middle) and the resulting DoS $\sigma_1(\cdot) - \sigma_2(\cdot)$ with $\gamma = 1$(right). The vertical dashed line marks the turning point at $x^* = 6.01$ as a function of c_1, c_2, s_1, s_2.

2.2 Introducing stochastic trends in the nonlinear panel model

CO_2 emissions are mostly driven by economic development, originating from the fuels that generate electricity, power automobiles, ships and aircraft, and fuel industrial activity. As a result, economic growth has been closely tied to a rise in greenhouse gas emissions throughout modern economic history. However, this relationship changes over time. We are witnessing steady improvements in the energy intensity of economic growth (i.e., less energy is required to produce a unit increase in GDP). Recently, a dramatic rise in clean energy deployment has shown a growing divergence between GDP growth and CO_2 emissions in most economies around the world.

These developments cannot be captured within our static EKC model, as changes in CO_2 can only be channelled through changes in GDP. With the advent of energy efficiency and clean energy, GDP can still grow but with a lower CO_2 emission level. It is challenging to acquire trustworthy macroeconomic indicators that consistently reflect these more recent technological developments across a diverse panel of countries. Therefore, we will allow a selection of static coefficients in our model to be replaced by dynamic processes so they can adapt (slowly) over time.

The fixed effect μ_i in our static model (2.1) represents the base level of CO_2 emissions in country i, corrected for economic activity through our nonlinear EKC decomposition mechanism. The strictly static nature of this fixed effect is highly restrictive in the context of the EKC. The level of CO_2 emissions depends on economic activity but also on the underlying energy mix of a country. Whether the economic output of a country relies primarily on energy from coal or gas is reflected by the different fixed effects μ_i across countries. However, many countries have witnessed huge transitions in their energy resources, mostly moving towards energy mixes that emit lower levels of CO_2. To account for these major, unobserved structural transitions, we generalize the static fixed effects by introducing stochastically time-varying country trends.

The dynamic extension of model (2.1) involves replacing the static fixed effect μ_i of country i with the time-varying two-way effect $\mu_i + \tau_{it}$, where τ_{it} is a simple dynamic random walk process given by

$$\tau_{i,t+1} = \tau_{it} + \eta_{it}, \tag{2.3}$$

where initial value $\tau_{i,1}$ is treated as a diffuse prior, which is similar to assuming it is an unknown coefficient, and η_{it} is assumed to be an IID noise term with mean zero and variance σ_η^2, for $i = 1, \ldots, N$ and $t = 1, \ldots, T$, and is assumed to be independent of the observation noise ε_{js}, for all $j = 1, \ldots, N$ and $s = 1, \ldots, T$.

Apart from the economic motivation, the dynamic extension of the nonlinear EKC model also directly addresses the valid econometric criticisms raised by Wagner (2015) and Wagner et al. (2020), who have demonstrated that nonlinear regression approaches applied to non-stationary variables may produce unreliable results. Static regressions that leave the non-stationary features in the residuals inherently produce spurious estimation results. By explicitly including the stochastic trends τ_{it} as the non-stationary processes defined in (2.3), we treat the non-stationary features in the data directly as part of the structural model. We analyze all components within our dynamic nonlinear country panel model simultaneously, effectively separating the deterministic EKC function from stochastic technological and policy shocks.

3 Parameter estimation and signal extraction

3.1 Parameter estimation for the static model

The empirical evaluation of the static EKC model requires estimating the structural shape parameters alongside the country-specific fixed effects. This task is relatively straightforward, despite the highly nonlinear relationship between the economic output x_{it} and the environmental impact y_{it}.

First, we collect all static parameters to be estimated in the vector ψ

$$\psi = (\mu_1, \ldots, \mu_N, \gamma, c_1, s_1, c_2, s_2, \sigma_\varepsilon^2)'. \tag{3.1}$$

For any given parameter vector ψ, the error term ε_{it} is entirely determined by the observables y_{it} and x_{it}. Second, the goal is to find the parameter values that best match the observed relationship between the income and emissions variables. The model is fitted by minimizing the sum of squared errors between the predicted values from the structural curve and the actual observed emissions,

$$S_\varepsilon(\psi) = \frac{1}{NT} \sum_{i=1}^{N} \sum_{t=1}^{T} \varepsilon_{it}^2. \tag{3.2}$$

This objective function is minimized with respect to ψ. Given the specification of the difference-of-sigmoids formulation, this constitutes a nonlinear least squares (NLS) problem and is carried out via the numerical minimization of $S_\varepsilon(\psi)$ using standard optimization algorithms.

3.2 Parameter estimation for the dynamic model

The estimation of parameters in models (2.1) and (2.3) requires the Kalman filter to treat the time-varying stochastic trends τ_{it} for each country i. Although the model is nonlinear in nature, we can still use the Kalman filter without relying on approximations. For this purpose, we employ a penalized profile log-likelihood approach based on a partial state-space representation. This strategy allows us to handle the nonlinearity of the component EKC while efficiently accounting for the unobserved, non-stationary stochastic trends.

For a given value of the parameter vector ψ, we can define and compute the variable

$$z_{it} = y_{it} - \gamma \left[\sigma_1(x_{it}; c_1, s_1) - \sigma_2(x_{it}; c_2, s_2) \right], \qquad i = 1, \ldots, N, \quad t = 1, \ldots, T, \tag{3.3}$$

and consider the model for z_{it}:

$$z_{it} = \mu_i + \tau_{it} + \varepsilon_{it}, \qquad \tau_{i,t+1} = \tau_{it} + \eta_{it}, \tag{3.4}$$

which is effectively a multivariate local level model as discussed in Harvey (1989). This model can be statistically treated by the Kalman filter; see Durbin and Koopman (2012).

To account for the large country panel dimension and the corresponding numerous fixed effects and random walk processes, we adopt a profile log-likelihood approach as follows. In effect, for the transformed panel dataset z_{it}, given a candidate value for the structural parameters, the static fixed effects can be estimated analytically by their associated sample means defined by

$$\widehat{\mu}_i = \frac{1}{T} \sum_{t=1}^{T} z_{it}, \tag{3.5}$$

and the demeaned transformed data is computed as $z_{it}^* = z_{it} - \widehat{\mu}_i$, for each $i = 1, \ldots, N$. The estimates $\widehat{\mu}_i$ can be interpreted as the base level of CO_2 emissions of country i in year 1, allowing us to concentrate out the intercepts from the optimization routine.

Subsequently, we cast the multivariate local level model for z_{it}^* into a linear state-space form to be statistically treated by the Kalman filter; see Durbin and Koopman (2012). Let z_t^* be the $N \times 1$ vector of observations at time t. The observation and state equations are given by

$$z_t^* = Z_t \alpha_t + \varepsilon_t, \quad \varepsilon_t \sim N(0, H_t), \tag{3.6}$$

$$\alpha_{t+1} = T_t \alpha_t + R_t \eta_t, \quad \eta_t \sim N(0, Q_t), \tag{3.7}$$

where α_t is the $N \times 1$ state vector containing the stochastic trends $(\tau_{1t}, \ldots, \tau_{Nt})'$. The system matrices are defined as $Z_t = T_t = R_t = I_N$, while the variance matrices are $H_t = \sigma_\varepsilon^2 I_N$

and $Q_t = \sigma_\eta^2 I_N$. The Kalman filter delivers the one-step-ahead prediction errors and their corresponding variances, defined as

$$v_{it}(\psi) = y_{it} - E(y_{it}|Y_{t-1};\psi), \qquad F_{it}(\psi) = \mathrm{Var}(y_{it}|Y_{t-1};\psi), \tag{3.8}$$

for $i = 1, \ldots, N$ and $t = 1, \ldots, T$, where $Y_t = \{y_{11}, \ldots, y_{1t}, \ldots, y_{N1}, \ldots, y_{Nt}\}$. This specification allows us to recursively compute the log-likelihood function $\mathcal{L}_{Kalman}(\psi)$. Although we have not made Gaussian assumptions, we adopt the (quasi-)log-likelihood function as given by

$$\mathcal{L}_{Kalman}(\psi) = -\frac{NT}{2}\log 2\pi - \frac{1}{2}\sum_{i=1}^{N}\sum_{t=1}^{T}\left(\log F_{it} + \frac{v_{it}^2}{F_{it}}\right). \tag{3.9}$$

To allow a feasible handling of the dynamic (unobserved stochastic trends) and nonlinear (EKC) features in our model simultaneously and efficiently for the parameter estimation of ψ, we minimize the negative log-likelihood function $\mathcal{L}_{Kalman}(\psi)$, augmented with penalty terms to ensure identification. A common challenge in dynamic decomposition models is the simultaneous identification of multiple components. In our case, during the estimation process, parameter values can be visited that allow the flexible stochastic trend to absorb all variations embedded in the EKC part of the model. To prevent this danger of 'overfitting' and to preserve the role and interpretation of the EKC, we introduce two regularization penalties. Hence, the objective function is defined as

$$S_v(\psi) = -\mathcal{L}_{Kalman}(\psi) + \lambda_{snr}P_{snr} + \lambda_{ekc}P_{ekc}, \tag{3.10}$$

where the two penalty terms are given by

$$P_{snr} = \delta(\sigma_\eta > 0.5\sigma_\varepsilon)(\sigma_\eta - 0.5\sigma_\varepsilon)^2, \qquad P_{ekc} = \delta(\gamma < 1.0)(1-\gamma)^2. \tag{3.11}$$

The function $\delta(\cdot)$ acts as an indicator function where $\delta(\text{true}) = 1$ and $\delta(\text{false}) = 0$, while λ_{snr} and λ_{ekc} determine the strength of each penalty. The term P_{snr} enforces a soft constraint on the signal-to-noise ratio, ensuring that technological change remains a gradual process, while P_{ekc} forces the optimizer to search for a significant structural relationship. We set $\lambda_{snr} = \lambda_{ekc} = 10^6$ in all specifications reported below.

Parameter estimation is carried out by minimizing $S_v(\boldsymbol{\psi})$ with respect to the parameter vector ψ via the quasi-Newton numerical penalized minimization method L-BFGS-B developed by Byrd et al. (1995). It is worth noting that the development of our estimation procedure does not involve any approximation.

3.3 Stochastic trend extraction

Once the unknown parameters in the vector ψ are estimated for a given dynamic panel model, we obtain $\widehat{\psi}$ and are able to estimate the unobserved trend components τ_{it}, for all countries $i = 1, \ldots, N$, by means of the Kalman filter and smoother. The Kalman filter is already used during the parameter estimation process, as it effectively evaluates the objective function $S_v(\psi)$. The Kalman filter is a forward filter. The storage of the one-step ahead prediction errors and their corresponding variances (v_{it} and F_{it}) allows us to apply a backward smoothing algorithm that evaluates the conditional means and variances defined as

$$\widehat{\tau}_{it}(\psi) = E(\tau_{it}|Y_T;\psi), \qquad V_{it}(\psi) = \mathrm{Var}(\tau_{it}|Y_T;\psi), \tag{3.12}$$

at $\psi = \widehat{\psi}$, simultaneously for all countries $i = 1, \ldots, N$ and $t = 1, \ldots, T$, where $Y_T = \{Y_1, \ldots, Y_T\}$ represents the full sample information.

By combining these smoothed state estimates with the concentrated static fixed effects, the resulting time-varying baseline estimates, $\widehat{\mu}_i + \widehat{\tau}_{it}$, can show how the base emissions effect for each country is evolving over time. This Kalman filtering and smoothing method operates for a given state-space model representation with the observation and state equations defined in (3.4) and (2.3). Note that this state-space model relies on the transformed data z_{it}, as defined in equation (3.3). Derivations and further mathematical details of the Kalman filter, smoothing algorithms and trend extraction are provided in Durbin and Koopman (2012, Chapter 4).

3.4 Bootstrap method for computing standard errors

For the computation of standard errors, confidence intervals, and test statistics in our dynamic nonlinear panel model, we adopt the bootstrap method proposed by Stoffer and Wall (1991). Given that the input of the Kalman filter is z^*_{it} rather than y_{it}, the model contains a nonlinear regression function and it is a dynamic panel model, various modifications need to be made. We discuss the implementation of the bootstrap method in detail in the Appendix A.3. However, the general idea of generating many bootstrap replicates of the data via the re-sampling of (pre-whitened, standardized) prediction errors, and re-estimating the parameter vector in the same way (using L-BFGS-B and the two penalty terms) but now for each bootstrap panel data set remains valid. In this way, we obtain $B = 500$ bootstrap estimates of the parameter vector from which we can construct standard errors and confidence intervals for all parameters, but also for any quantity that is a function thereof.

4 Empirical study: the global EKC

4.1 Data resources

We analyze a panel data set of 15 major economies over the period 1980–2019 ($N = 15$ and $T = 40$). These countries account for more than 75% of both global GDP and global greenhouse gas emissions according to OECD (2017), capturing the 'critical mass' of the global economy. The panel includes advanced economies (comprising the G7 nations plus Australia) and emerging economies (E7 nations).

The time span is chosen to ensure data reliability and consistency with the evolution of international climate policy. It provides a balanced number of observations around the adoption of the Kyoto Protocol in 1997 and captures different stages of industrialization and technological progress from 1980 onward. Observations after 2019 are excluded to avoid the temporary disruptions to GDP and emissions caused by the COVID-19 pandemic. For Germany, the standard practice in macroeconometrics is adopted, and pre-1990 data refer only to West Germany to preserve structural continuity.

The two core variables, x_{it} and y_{it}, are obtained from the Our World in Data (OWID) database, Roser et al. (2024), which compiles data from established international sources and allows for full replication. The economic variable, x_{it}, is the natural logarithm of GDP per capita, based on World Development Indicators data World Bank (2024) and measured in 2021 constant international dollars using purchasing power parity (PPP) conversion rates. The environmental variable, y_{it}, is the natural logarithm of per-capita CO_2 emissions, measured in metric tons and sourced from the Global Carbon Budget Friedlingstein et al. (2025). It includes emissions from fossil-fuel combustion and industrial processes but intentionally excludes emissions from land-use change. Both series are expressed in per capita terms to ensure comparability between countries and constitutes a panel covering the 1980–2019 period.

Figure 2 presents the historical trajectories of these series. The left panel displays the log of per-capita CO_2 emissions, and the right panel the log of real GDP per capita. Solid lines represent the advanced economies and dashed lines the emerging ones.

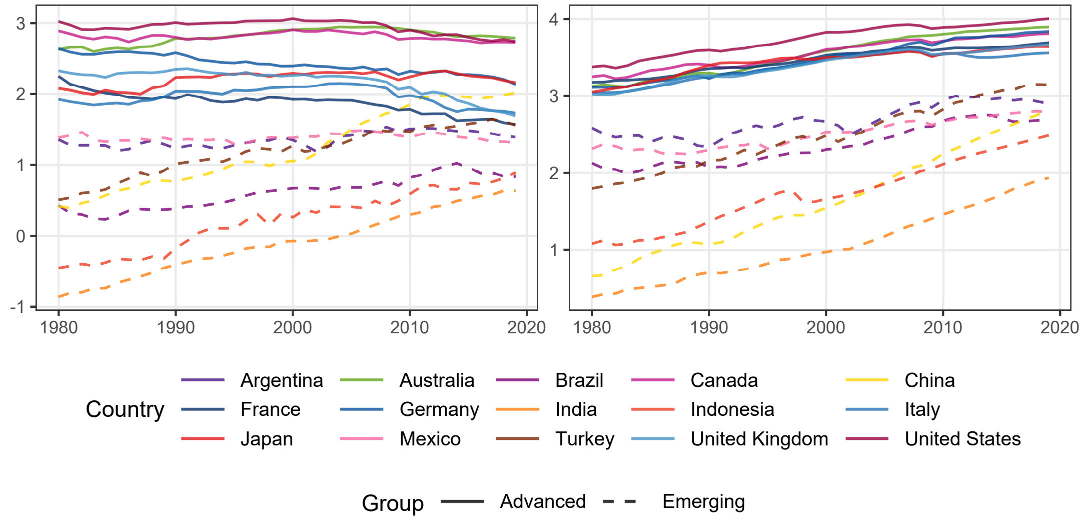

Figure 2: Evolution of Log(CO_2 per-capita) (left) and Log(GDP per-capita) (right).

4.2 Empirical results of static EKC model for each country (single equation)

As a baseline exploratory step, we first estimate the static difference-of-sigmoids (DoS) model for each country individually. Figure 3 presents the time series observations for log CO_2 per capita against their corresponding log GDP per capita, together with the country-specific fits from the static nonlinear regression model (single equation). These results show highly heterogeneous trajectories for the individual fits of the 15 countries. Developed economies such as the United Kingdom, United States or France display visibly inverted U-shaped patterns, which are indicative of a green transition. Emerging economies such as India, Indonesia or Brazil remain on a steep upward trajectory. However, while the fit of these single equation regressions might appear adequate, a detailed inspection of the estimated parameters reveals severe econometric identification issues and parameter degeneracy.

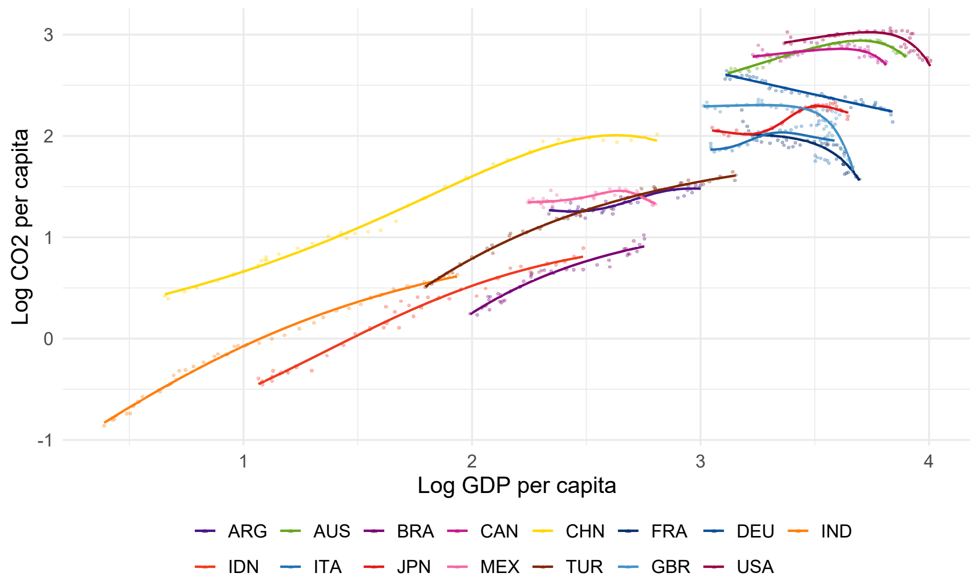

Figure 3: Country-specific EKC fits from nonlinear regression model (single equation).

Table 1 displays the estimated parameters for $\mu, \gamma, c_1, c_2, s_1, s_2$ from the nonlinear regression model for each country. Since the highly nonlinear DoS function requires estimating six structural parameters using only the limited time-series of a single country, the optimization algorithm suffers from severe overfitting, capturing idiosyncratic historical shocks rather than the underlying structural EKC relationship.

We observe three major mathematical anomalies that make the EKC estimates of little economic relevance for various countries. First, the collapsing of turning points of the two sigmoids ($c_1 = c_2$) occurs for several economies, including Argentina, Australia, Germany, Italy and Mexico. This collapse implies that the economic growth and green transition phases trigger at the same point, violating the EKC interpretation of 'grow first, clean later'. Second, the numerical minimization algorithm for the nonlinear regression hits the absolute lower bound of 0.00001 for the slope coefficients s_1 and s_2. For instance, the economic growth slope (s_1) approaches zero for France and Germany, which falsely implies that emissions do not grow as a result. However, when the green transition slope (s_2) hits zero for emerging economies such as Brazil, India, Indonesia or Turkey, it can be concluded correctly that the green transition has not yet started. In this case, the green sigmoid reduces to a constant and, hence, c_2 cannot be identified from the data. Third, some implausible estimates for the amplitude parameter γ are obtenied and these vary heavily among countries. The estimate ranges from 1.70 for Argentina to a value as large as 38.8 for France. In such cases as France, the algorithm forces the unity-scaled sigmoid to capture the negative trend breaks in CO_2 emissions due to the French nuclear rollout. Hence, the relevance of the model for the EKC is lost as a result. Furthermore, these results can be dismissed due to overfitting, in which we use a flexible specification to only fit $T = 40$ yearly observations.

Table 1: Estimated parameters for the static univariate model.

Country	μ	γ	c_1	c_2	s_1	s_2
Argentina	1.3670	1.7030	2.7050	2.7060	6.7200	4.9870
Australia	1.3980	4.1400	4.1940	4.1950	0.8120	7.1500
Brazil	-6.6580	15.7440	0.2780	-	1.5870	0.0000
Canada	-3.4430	11.3960	1.1760	4.1270	0.0900	12.2770
China	-0.1900	8.3760	3.1270	3.5050	1.0090	2.3350
France	-17.3500	38.7560	-	4.2660	0.0000	7.7100
Germany	2.9070	6.3320	-	2.5200	0.0000	0.3240
India	-1.3990	4.8690	0.0000	-	1.2200	0.0000
Indonesia	-0.1150	2.3150	1.3670	-	1.9550	0.0000
Italy	1.9110	19.3870	3.2390	3.2400	10.2080	10.0220
Japan	2.1000	2.3300	3.3890	3.4060	11.6980	9.0760
Mexico	1.3430	18.2080	2.7380	2.7390	12.7410	12.9880
Turkey	-4.7370	13.3000	0.0000	-	1.1920	0.0000
United Kingdom	-4.9830	14.4860	2.5830	3.9160	0.0200	12.0890
United States	-1.0500	7.8250	3.2170	4.2980	0.2000	9.3280

These results strongly confirm that a single equation analysis based on the static EKC regression model is not able to reliably capture the nonlinear features of the EKC and the corresponding dynamic features. This analysis provides country-specific curves, but is based on spurious estimates that do not capture the economic growth and green transition stages implied by the EKC. Consequently, we next consider the estimation of the EKC by pooling coefficients across all countries within a panel data modeling framework.

4.3 Empirical results of static EKC nonlinear panel model (fully pooled)

To overcome the severe parameter degeneracy and overfitting observed in single equation regressions, our second step involves estimating a standard pooled static model with country-specific fixed effects μ_i and a common DoS function in model equation (2.1). This approach is similar to many of the traditional methods prevalent in the EKC literature.

Figure 4 presents the yearly observations of log CO_2 against log GDP, together with the estimated pooled EKC function plus the estimated country-specific fixed effects, which are displayed only for the range of observed log GDP values for each of the 15 countries. In contrast to the heterogeneous and erratic EKC single regression fits, the basic pooled static model provides strictly parallel trajectories for the EKC in each country. The EKC is constrained to have the exact same nonlinear shape for each country, it differs only because of the input values of GDP (y-axis) and the vertical shifts (fixed effects).

Although the pooling of EKC parameters stabilizes the fit of the EKC function by leveraging cross-sectional variation, pooling also imposes a somewhat rigid trajectory of the EKC for all countries; see Figure 4. The estimated EKC parameters for this deterministic transition include the global economic output threshold $c_1 = 3.24$ and the global green transition threshold $c_2 = 3.97$, being larger than the estimate of c_1. The shifts of the fitted EKC for all countries reflect the different fixed effect estimates and successfully capture the baseline differences in per capita emissions levels. However, a closer inspection reveals that the EKC fit is too smooth and shows a poor fit, especially for the G7 countries. We therefore turn to the residuals from this static nonlinear EKC panel model. On the basis of a graphical inspection, we can already conclude that the model does not capture the time series features very well. Many residual series show trending behaviour, especially those of the G7 countries.

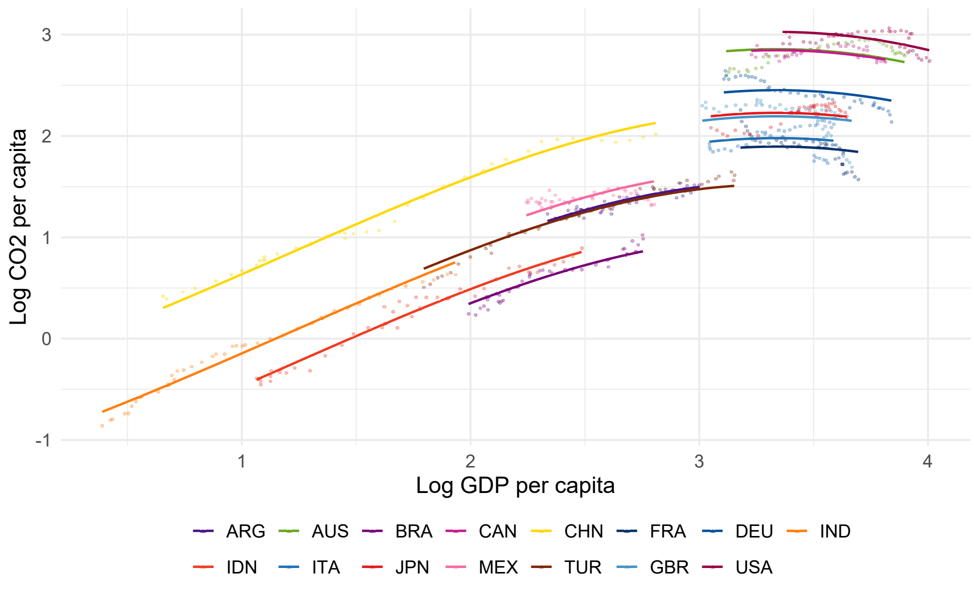

Figure 4: Country-specific EKC fits based on the static panel model with fixed effects.

A more formal diagnostic analysis for the residual series exposes a fundamental econometric flaw that echoes the criticism raised by Wagner (2015). In our context, the criticism is as follows. The time series in Figure 2 may suggest that for each country, the two time series log CO_2 and log GDP are cointegrated, that is, they appear to share a common trend. However, the nonlinear transformation of log GDP implied by the DoS function in the model (2.1) may *not* be cointegrated with log CO_2. This is confirmed by the residual series that show clear evidence of non-stationary features. This evidence is collected in Figure 5, which consists of a summary of residual diagnostic tests for individual countries. It contains four plots with first-order autocorrelations and p-values for the Ljung-Box, augmented Dickey-Fuller (ADF) and Shapiro-Wilk tests. We firmly reject the white noise assumption for almost all residual series, as most diagnostic values fall far outside their theoretical bounds, as indicated by the dashed lines. First, the residuals exhibit severe first-order serial correlation, with many sample autocorrelations close to 1.0. Also, we overwhelmingly reject the Ljung-Box null hypothesis of white noise across the entire panel. Second, the individual ADF tests indicate a widespread failure to reject the null hypothesis of a unit root. For most G7 countries, the static model systematically over-predicts the emissions because it cannot account for its trending behavior.

We have also considered the inclusion of a deterministic trend for each country, in model (2.1) replacing μ_i by $\mu_i + \delta_i t$ where δ_i is the slope coefficient of the trend line. In the Appendix B.1, we present the estimation results from this extended model. The estimates of δ_i are negative for all advanced economies, while positive for most emerging economies. The residual diagnostics have somewhat improved but, crucially, the null hypotheses of white noise and of a unit root can still not be rejected for any of the fifteen countries.

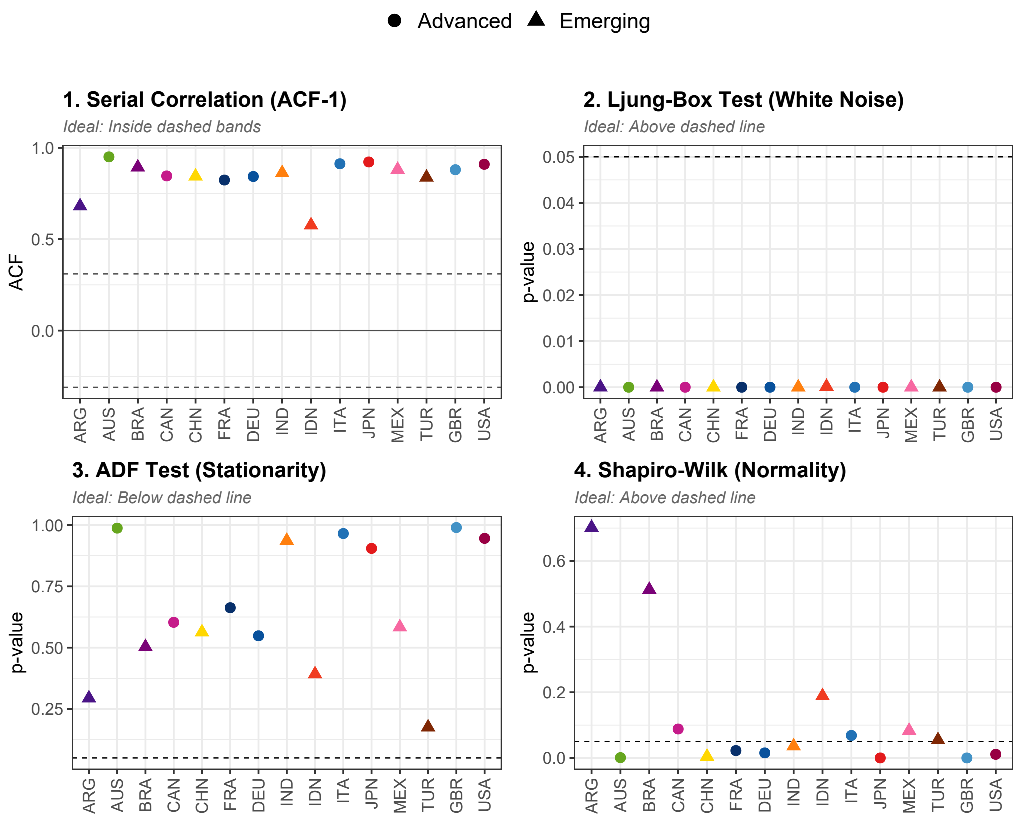

Figure 5: Residual diagnostics panel (fixed effects).

We can conclude from the residual diagnostics that a static formulation of the EKC model can suffer from spurious regression issues. In other words, the model fails to capture latent, unobserved trends which may be due to external government investment programs, but also due to technological developments, evolving policy regimes or other institutional and societal changes. We therefore consider our base model with the inclusion of country-specific stochastic trends as specified in model equation (2.3). In this way, we can account for country-specific events such as the persistent energy transition to nuclear in France, the 'dash for gas' transition in the UK, and the industrial complex transition in the former East Germany. These transitions can be regarded as external phenomena, as they have not been motivated by green policies nor by the EKC interpretation of 'grow first, clean later'. Hence, we let both the DoS function and the stochastic trends be present in our dynamic EKC model.

4.4 Empirical results of dynamic nonlinear panel models

We replace fixed effects in the static model by country-specific stochastic trends in (2.3) mainly to counter spurious regression issues. However, the stochastic trends can also be viewed as proxies of omitted variables such as energy mix, technology, and regulatory costs that have an impact on emissions in the medium and/or long-term. In this way, we also treat endogeneity issues related to the EKC as discussed, for example, in Stern (2004). With the introduction of the DoS function in the EKC model, we possibly reduce "functional-form" endogeneity. With the introduction of stochastic trends, the estimation process as described in Section 3.2 relies on the Kalman filter that by construction introduces lagged dependent variables in the filtering equations. Hence, the Kalman filter effectively introduces instrumental variables during estimation since lagged (dependent) variables are often advocated and used as such. The estimation results are discussed next for different panel selections: for all fifteen countries, for emerging economies (E7), and for advanced economies (G7 plus Australia). Table 2 reports the parameter estimates for the three different panel selections, alongside with our preferred panel model, for all countries but with a regional EKC specification. The table also reports the estimates of the contrast $c_2 - c_1$ and the implied turning points of the EKC which are both key to the interpretation of our findings. We further report the maximized penalized log-likelihood values and, where appropriate, the standard errors obtained from the bootstrap procedure described in Section 3.4.

Table 2: Parameter estimates for different model specifications, with standard errors where appropriate.

	Global		E7	E7+G7	G7	Regional	
	Est.	SE	Est.		Est.	Est.	SE
γ	3.715	1.635	9.132		6.092	5.072	1.308
c_1	1.106	0.353	1.461		4.215	0.699	0.353
c_2	4.564	0.379	5.518		4.585	4.935	0.391
c_2^{Eur}						4.492	0.269
s_1	1.040	0.215	0.470		0.179	0.777	0.172
s_2	4.501	1.204	1.007		5.000	3.492	1.167
$c_2 - c_1$	3.457	0.539	4.057		0.370	4.237	0.535
$c_2 - c_2^{Eur}$						0.443	0.206
Turning-point	3.631	0.099	–		3.645	3.779	0.116
for Eur						3.406	0.095
gap Eur						0.373	0.107
Log-likelihood			459.41		516.43		
	984.83			975.84		992.39	

Note: Parameter estimates (Est.) are reported for three model specifications: full panel (Global), panel of emerging economies (E7), panel of advanced economies (G7) plus Australia, and full panel with a different activation c_2 for Europe (Regional). Standard errors (SE) are reported and obtained from the bootstrap method described in Section 3.4 based on $B = 500$ synthetic parameter estimates; they are not reported for the E7 and G7 specifications, see discussion in the text. Turning points are obtained as described in Section 2.1. The maximized, penalized log-likelihood values are reported (including the sum of E7 and G7).

A comparison of the estimation results for the separate models reveals the challenges of estimation. The E7 model captures the early industrialization phase accurately but lacks sufficient data on the post-transition downturn, resulting in a relatively high (delayed) green transition activation ($c_2 = 5.52$) and a flattened transition shape ($s_2 = 1.01$). Conversely, the G7 model captures the decarbonisation phase but lacks data on early industrialization, leading to an artificially delayed economic activation ($c_1 = 4.22$) and a flattened economic slope ($s_1 = 0.18$). The amplitude parameter (γ) inflates from 3.72 in the global model to 9.13 and 6.09 in the separate E7 and G7 models, respectively. These results illustrate that the optimization algorithm attempts to fit the complete DoS curve over the whole range of GDP values with limited observations. However, the estimates of observation noise scale σ_ε and the trend scale σ_η remain roughly constant across the three specifications, near 0.03 and 0.02, respectively. This stability in the scale parameters indicates that the divergence between models is mostly due to the estimation of the DoS function, rather than the stochastic trends.

The E7 and G7 models show that identifying the full EKC trajectory requires data across all countries to provide information on the different stages of economic development. This lack of identification also explains two omissions in Table 2. We do not report standard errors for the E7 and G7 specifications, since bootstrap inference is not informative for a model that is only partly identified from the data at hand. Nor do we report a turning point for the E7 model: its structural curve attains its maximum at the upper end of the income range observed for those countries, so the model places the emissions peak just beyond the incomes they have reached rather than within the sample.

Figure 6 shows the structural curves for the three models. To explicitly isolate the pure nonlinear relationship, the data points are the observed emissions detrended by the estimated stochastic trends (τ_{it}) which we have obtained from the Kalman filter and smoother. These plots scatter log CO_2 emissions against log GDP and show the fit of the DoS function captures the detrended data accurately. Note that the location and scale of the y-axes are not linked across the three models, as they are subject to baseline differences (fixed effects) and to different trend estimates. No turning point is marked for the E7 model, for the reason given above. The plots also show that our framework is flexible and effective in dealing with missing information for different developmental stages.

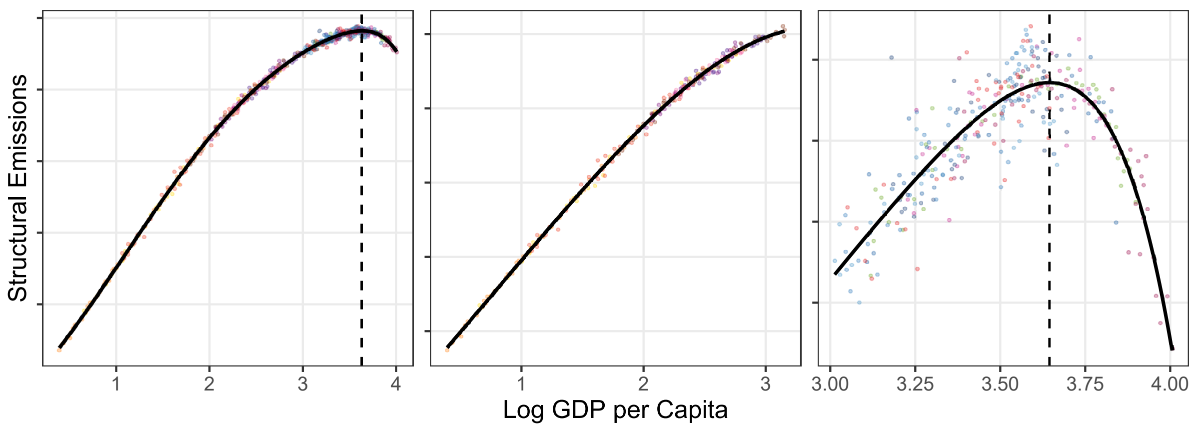

Figure 6: Structural curve estimates for the Global (left), E7 (middle) and G7 (right) panel models. Vertical dashed lines mark the estimated turning points reported in Table 2.

While the global dynamic panel model has successfully extracted the nonlinear EKC by pooling the related parameters over all countries, imposing a single green transition activation coefficient (c_2) for all 15 countries remains somewhat restrictive. From an econometric perspective, forcing a single activation point ignores the cross-country heterogeneity of the green transition. From an economic perspective, advanced European nations share a distinct institutional and policy landscape, characterized by earlier industrial maturity and highly coordinated supranational environmental frameworks, such as the European Union Emissions Trading System (EU ETS) and early Kyoto Protocol commitments. In particular regarding environmental policies, non-European countries are less subject to such regulatory constraints in economic activity. To accommodate this institutional feature for European countries without sacrificing the pooling of the remaining parameters in our model, we introduce a separate European activation parameter c_2^{Eur}, constraining c_1, s_1 and s_2 to be common across countries, so that the green transition may activate at a different level in Europe.

As shown in Table 2, the introduction of this single parameter shift improves the model's fit, increasing the maximized penalized log-likelihood from 984.83 in the global model to 992.39 in the regional specification. The estimates validate our hypothesis: the European bloc initiates its green transition at an activation threshold of $c_2^{Eur} = 4.492$, noticeably earlier than the rest of the world ($c_2 = 4.935$). The bootstrap confirms this difference: the contrast $c_2 - c_2^{Eur}$ has a 95% confidence interval of $[0.266, 1.132]$ and is positive in every replication.

Figure 7 presents the EKC fits for this dynamic panel model. The scatter points show the detrended data obtaind by subtracting $\widehat{\mu}_i + \widehat{\tau}_{it}$ from the observed data. The fit is accurate for both the global EKC and its European variant. The European curve peaks at $x^* = 3.41$ against 3.78 for the rest of the world, a gap of 0.37 log points of GDP per capita, confirming that Europe initiates the green transition at a significantly earlier level of economic output. After introducing the European parameter shift, our dynamic EKC model has successfully accommodated the most prominent source of regional structural heterogeneity while still leveraging the full panel to robustly identify the global EKC.

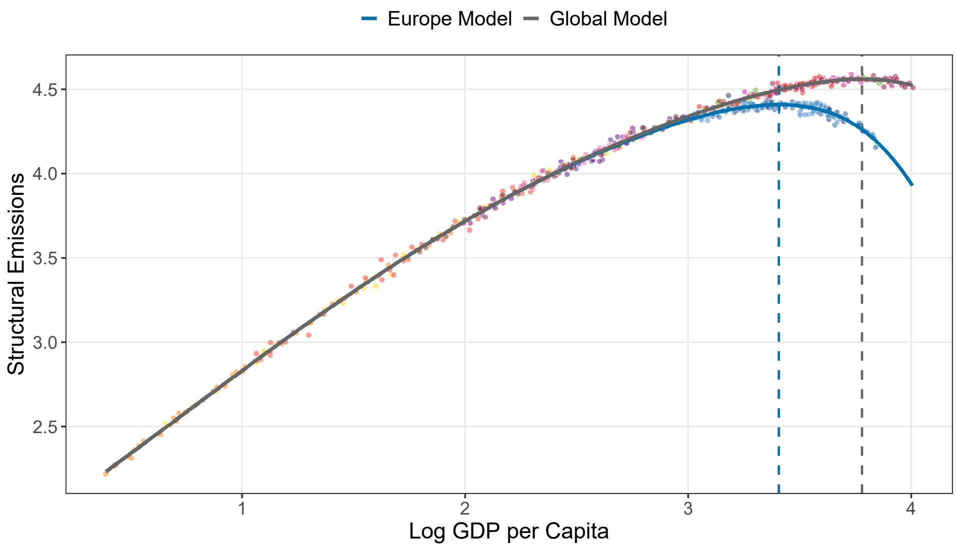

Figure 7: Structural emissions curves by region. Vertical dashed lines mark the estimated turning points reported in Table 2.

A crucial advantage of introducing country-specific stochastic trends and adopting state-space methods for extracting these trends is the ability to explicitly capture the non-stationary features in the data directly, thereby avoiding the issues related to spurious regressions. On the other hand, introducing these flexible trend formulations into the model may also lead to issues related to overfitting. Figure 8 displays the estimated stochastic trends τ_{it} obtained from the Kalman filter and smoother. The estimated trends are displayed over the 1980–2019 period for each of the 15 countries. These extracted trends capture trajectories for specific countries that we can interpret as external factors. For example, persistently declining emissions take place in France in the aftermath and ongoing implementation of the Messmer plan, in the United Kingdom in the post-1990 period known as the 'dash for gas' policy, and in Germany during its ongoing restructuring of the old industrial complex in the former East Germany. For most other countries, the trends are relatively flat and stable, with some fluctuations related to temporary shocks due to, for example, the collapse of the Soviet Union and the fluctuating energy intensity dynamics in rapidly growing economies such as China and India.

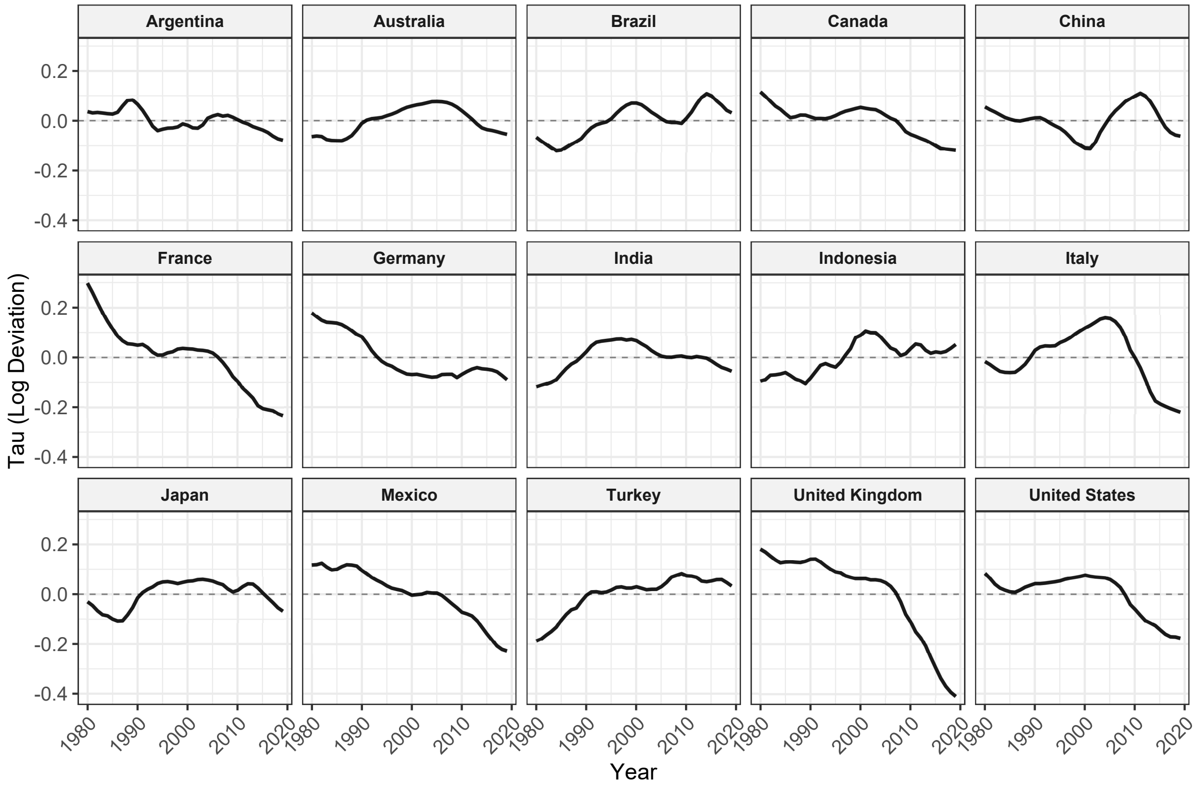

Figure 8: Estimated stochastic trends by country.

To explore the cross-sectional dependence of these extracted stochastic trends, we estimate a Dynamic Factor Model following the approach of Peña and Box (1987). The distribution of the estimated loadings for the first common factor is presented in Figure 9. The colour gradient illustrates the magnitude and direction of these loadings, where darker blue indicates a strong positive correlation with the factor (typical of advanced economies) and red indicates a negative correlation. Countries depicted in light grey were not included in the sample.

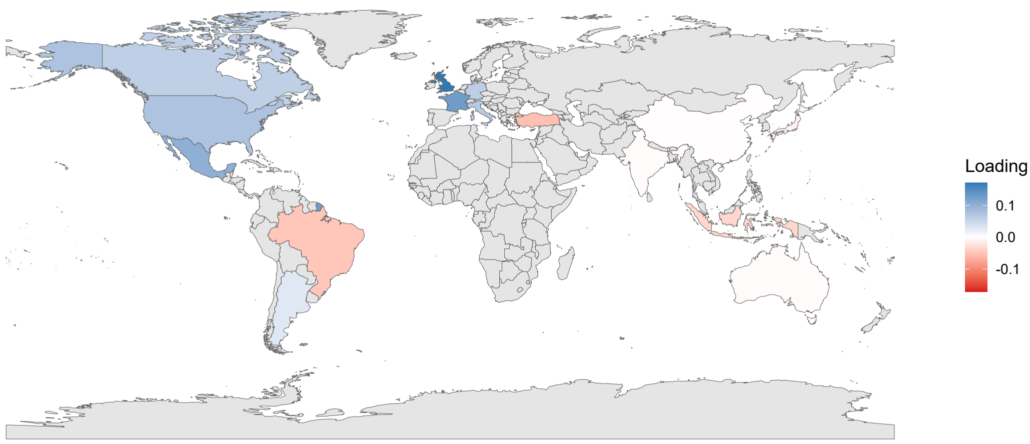

Figure 9: Loadings for the first dynamic factor from trends in Figure 8.

We next study the residuals of our preferred model. Table 3 presents the estimated country-specific fixed effects together with the residual diagnostic tests. In stark contrast to the static fixed-effects specification, the ADF tests now reject the unit root null hypothesis at the 5% level for the vast majority of the panel, confirming that the residuals are stationary. Furthermore, the Ljung-Box and Shapiro-Wilk tests show substantial improvements, indicating that the error terms broadly approximate stationary white noise behaviour. These diagnostic results validate that our preferred dynamic EKC model successfully identifies an economically relevant global EKC, the U-shaped relation between economic output and CO_2 emissions. We have shown that the residuals are sufficiently close to stationarity.

Table 3: Country-specific fixed effects and residual diagnostics (Final Regional Model).

Country	$\hat{\mu}_i$	Ljung-Box (p-val)	ADF Test (p-val)	Shapiro-Wilk (p-val)
Argentina	-2.811	0.1360	0.0100**	0.4764
Australia	-1.694	0.0482	0.0111**	0.3807
Brazil	-3.354	0.0182	0.1252	0.7166
Canada	-1.708	0.4584	0.0100**	0.0576
China	-2.156	0.0023	0.1198	0.3941
France	-2.505	0.5906	0.0100**	0.0016
Germany	-1.929	0.4213	0.0100**	0.0516
India	-2.961	0.6991	0.0145**	0.6790
Indonesia	-3.254	0.5733	0.0100**	0.6170
Italy	-2.422	0.0636	0.0204**	0.2997
Japan	-2.286	0.0662	0.0185**	0.8535
Mexico	-2.679	0.6358	0.0100**	0.3968
Turkey	-2.844	0.9243	0.0100**	0.4701
United Kingdom	-2.203	0.6588	0.0886	0.2631
United States	-1.593	0.4127	0.0100**	0.4757

Note: Asterisks (**) denote rejection of the unit root null hypothesis at the 5% significance level.

In summary, the empirical evidence in this section strongly validates the deployment of state-space methods for obtaining a solid global EKC. By explicitly decomposing the emissions trajectory into a static DoS curve and country-specific stochastic trends, we address the spurious regression issues associated with traditional static panel estimations. Our final specification with an additional European parameter not only recovers a statistically valid EKC, but it also highlights critical heterogeneity among the countries. In particular, European economies initiated their green transition significantly earlier than the global average. Ultimately, this robust econometric identification confirms that while a fundamental developmental path exists, idiosyncratic technological and policy-driven shocks play an equally vital role in shaping a country's environmental trajectory.

5 Conclusions

This study proposes a dynamic panel model with a new functional specification for the Environmental Kuznets Curve (EKC), for a large group of countries. Instead of the usual quadratic specification, we represent the EKC as the difference of two sigmoid functions: one captures the increasing emissions due to economic growth, while the other captures the decreasing emissions due to the green transition. Furthermore, country-specific stochastic trends are added to the model to allow for external factors such as evolving changes in the energy mix, overall technological progress, and omitted variables. The EKC and the stochastic trends are treated simultaneously using state-space methods such as the Kalman filter and smoother. The parameters are estimated by maximum likelihood and standard errors are computed by a state-space bootstrap method.

This novel approach also addresses the challenges of treating cointegration in a nonlinear setting and the dangers of generating spurious EKC estimation results. In our empirical study, we analyze a panel of CO_2 emissions and GDP time series for 15 major economies (the G7 plus Australia and the E7) for the years 1980–2019. We have been able to identify a meaningful global EKC from the data. The global EKC provides a reasonable fit to European countries, but we find empirical evidence that they have initiated the green transition at a lower level of economic output. The model is sufficiently flexible to account for countries that are early adopters of green policies. Further extensions of the EKC model in several directions are planned for future research.

A Model specification and estimation

A.1 Analytical characterization of the turning point in a DoS

The deterministic EKC component, viewed as a function of (log) income $x \equiv x_{it}$, is

$$g(x) = \gamma\big[\sigma_1(x; c_1, s_1) - \sigma_2(x; c_2, s_2)\big], \qquad \sigma_j(x) = \frac{1}{1 + \exp[-s_j(x - c_j)]}. \tag{A.1}$$

The logistic satisfies $\sigma_j'(x) = s_j\, \sigma_j(x)[1 - \sigma_j(x)] \equiv s_j\, \phi_j(x)$, with $\phi_j := \sigma_j(1 - \sigma_j)$ being the symmetric and unimodal logistic density centred at c_j. Hence

$$g'(x) = \gamma\big[s_1\phi_1(x) - s_2\phi_2(x)\big], \tag{A.2}$$

and the first-order condition (FOC) $g'(x^*) = 0$, with $\gamma \neq 0$, is the equation

$$s_1\, \sigma_1(x^*)\big[1 - \sigma_1(x^*)\big] = s_2\, \sigma_2(x^*)\big[1 - \sigma_2(x^*)\big]. \tag{A.3}$$

Consequently the turning point depends only on $\theta = \{c_1, c_2, s_1, s_2\}$ and is invariant to the amplitude γ, to the fixed effects μ_i and to the trend terms. All these terms shift the level of g but not the location of its maximum. This isolates the four parameters that govern x^* and restricts its sampling uncertainty to the 4×4 block of $\widehat{\theta}$.

Differentiating (A.2) once more, we obtain

$$g''(x) = \gamma\,(s_1^2\phi_1\kappa_1 - s_2^2\phi_2\kappa_2) = \gamma\, D(x), \tag{A.4}$$

where $\kappa_j := 1 - 2\sigma_j$.

Proposition 1 (existence, concavity and uniqueness)**.** *Let $\gamma > 0$, $c_1 < c_2$ and $s_1, s_2 > 0$:*

(i) g attains a global maximum at some finite x^* with $g(x^*) > 0$.

(ii) g is strictly concave on (c_1, c_2).

(iii) If $g'(c_1) > 0 > g'(c_2)$, i.e, $s_1\phi_1(c_1) > s_2\phi_2(c_1)$ and $s_2\phi_2(c_2) > s_1\phi_1(c_2)$, then the global maximum $x^* \in (c_1, c_2)$ and is the unique critical point there.

Proof. (i) Since $c_1 < c_2$, $\sigma_2(c_1) = \sigma\big(s_2(c_1 - c_2)\big) < \frac{1}{2}$, so $g(c_1) = \gamma\big[\frac{1}{2} - \sigma_2(c_1)\big] > 0$. In addition, $\sigma_1, \sigma_2 \to 1$ as $x \to +\infty$ and $\to 0$ as $x \to -\infty$, so $g \to 0$ in both tails. Choosing M with $g(x) < g(c_1)$ for $|x| > M$ and $c_1 \in [-M, M]$, the Weierstrass theorem gives a maximum of g on $[-M, M]$ which is global, hence x^* exists with $g(x^*) \geq g(c_1) > 0$.

(ii) For every $c_1 < x < c_2$ we have $\sigma_1(x) > \frac{1}{2} > \sigma_2(x)$, so $\kappa_1 < 0 < \kappa_2$. Both terms of D in (A.4) are then negative and $g'' = \gamma D < 0$ throughout.

(iii) Since $\phi_j(c_j) = \frac{1}{4}$, (A.2) yields $g'(c_1) = \gamma\big(\frac{s_1}{4} - s_2\phi_2(c_1)\big)$ and $g'(c_2) = \gamma\big(s_1\phi_1(c_2) - \frac{s_2}{4}\big)$, so the stated inequalities are exactly $g'(c_1) > 0 > g'(c_2)$. By (ii), g' is strictly decreasing on (c_1, c_2) and therefore has a unique zero x^* there, a strict local maximum. As $g > 0$ on (c_1, c_2) (its endpoints are positive and g is concave) while $g \to 0$ in both tails, and a sign analysis of g' on $\mathbb{R} \setminus (c_1, c_2)$ shows its remaining zeros (when present) to be local minimum, x^* coincides with the global maximum of (i).

□

The condition in (iii) is a non-degeneracy (separation) requirement: it holds whenever the two transitions are distinguishable and fails only when they overlap so strongly that the peak migrates outside $[c_1, c_2]$. Existence and concavity, by contrast, require only $c_1 < c_2$. When $s_1 \neq s_2$ the exterior minimum just mentioned carries $g < 0$ and is never a competitor for the maximum.

If $s_1 = s_2 = s$, (A.3) reduces to $\phi_1 = \phi_2$, i.e. $\sigma_1(1-\sigma_1) = \sigma_2(1-\sigma_2)$. Since $u \mapsto u(1-u)$ is symmetric about $u = \frac{1}{2}$ and $c_1 \neq c_2$, $\sigma_1 = 1 - \sigma_2$. The latter gives $1 + e^{-s(x-c_1)} = 1 + e^{s(x-c_2)}$, hence $-(x - c_1) = x - c_2$. Finally,

$$x^* = \frac{c_1 + c_2}{2}, \qquad g(x^*) = \gamma \tanh\left(\frac{s\,(c_2 - c_1)}{4}\right). \tag{A.5}$$

This result also clarifies the role of γ. As the transitions separate, $c_2 - c_1 \to \infty$, the hyperbolic tangent tends to one and $g(x^*) \to \gamma$. Conversely, as they merge, $c_2 - c_1 \to 0$, the hyperbolic tangent tends to zero and $g(x^*) \to 0$. Thus γ is the maximal attainable amplitude of the EKC component (in log-CO_2 units), realized only partially when the two transitions overlap.

If $s_1 \neq s_2$, (A.3) has no closed-form solution. An approximation can nonetheless be derived from the shape of the two factors ϕ_j in the region where the maximum lies. By Proposition 1 the turning point lies in (c_1, c_2), where σ_1 has saturated ($\sigma_1 \to 1$) and σ_2 has not yet activated ($\sigma_2 \to 0$). Measure the saturation depth of each transition at x by

$$u_1 := s_1(x - c_1) > 0, \qquad u_2 := s_2(c_2 - x) > 0, \tag{A.6}$$

the two factors then take the exact form

$$\phi_j(x) = \sigma_j(1 - \sigma_j) = \frac{e^{-u_j}}{\big(1 + e^{-u_j}\big)^2}, \qquad j = 1, 2. \tag{A.7}$$

Deep in the tail u_j is large and e^{-u_j} is small, so we expand the denominator of (A.7) with the binomial series, obtaining

$$\phi_j(x) = e^{-u_j}\big(1 - 2e^{-u_j} + \cdots\big) = e^{-u_j} + O\big(e^{-2u_j}\big). \tag{A.8}$$

Substituting the leading terms of (A.8) into the balance condition $s_1\phi_1 = s_2\phi_2$ yields $s_1 e^{-s_1(x-c_1)} = s_2 e^{s_2(x-c_2)}$. Both sides are single exponentials, so taking logarithms linearizes the equation and gives a closed-form approximation

$$x^* \;\approx\; \frac{s_1c_1 + s_2c_2 + \ln(s_1/s_2)}{s_1 + s_2}. \tag{A.9}$$

The turning point is, to first order, a slope-weighted average of the two transition locations, plus a logarithmic correction $\ln(s_1/s_2)/(s_1 + s_2)$. It reduces exactly to the midpoint of (A.5) when $s_1 = s_2$. By (A.8) the relative error of each discarded factor is $O(e^{-u_j})$, so (A.9) is exponentially accurate when the transitions are well separated relative to their widths $1/s_j$ and only approximate under moderate overlap.

In the conventional quadratic EKC, the turning point results as $x^*_{\mathrm{q}} = -\beta_1/(2\beta_2)$, a ratio of two regression coefficients with no direct structural reading, and the curve is symmetric about its vertex. By contrast, (A.9) expresses the DoS turning point as a slope-weighted average of two parameters with explicit economic content: c_1, the income level at which emissions-intensive growth activates, and c_2, the level at which the green transition activates, plus a correction in their relative slopes. The implied hump is asymmetric (symmetric only if $s_1 = s_2$) and its shape is governed by $\{s_1, s_2\}$ independently of γ.

A.2 Sensitivity analysis on the penalties needed for the estimation

The objective function (see subsection 3.10 of the main paper) introduces two soft-constraint penalty terms: P_{snr} and P_{ekc} with tuning weights λ_{snr} and λ_{ekc}. These penalties are central to the identification strategy given that without them the stochastic trend can absorb the entire EKC signal. Here, some guidance on how the tuning parameters are chosen in practice and also some further investigation on how sensitive the estimated structural parameters are to alternative values of λ_{snr} and λ_{ekc} is reported.

In all the models' specifications reported in the paper (global, G7, E7 and regional models) are set to $\lambda_{snr} = \lambda_{ekc} = 10^6$, with the associated thresholds $\sigma_\eta \leq 0.5\,\sigma_\varepsilon$ for the signal-to-noise penalty P_{snr} and $\gamma \geq 1$ for the amplitude penalty P_{ekc}. It must be considered that once the weights are large enough to render the identifying restriction binding, then the estimates are insensitive to their precise magnitude, so a single value is used throughout. Additionally, the results obtained when investigating more deeply the role and the selection of the penalties are provided.

The final regional model is re-estimated across a grid of several penalty weights. Since the two penalties play different roles, each one is varied in turn. Table A.1 shows the results when the signal-to-noise weight λ_{snr} varies while keeping λ_{ekc} fixed. Table A.2 varies the amplitude weight λ_{ekc} at the chosen λ_{snr}. For each specification, the activation parameters c_1, c_2 and c_2^{Eur}, the amplitude γ, the log-variances, the implied signal-to-noise ratio $q = \sigma_\eta/\sigma_\varepsilon$ and the maximized log-likelihood values (with and without the penalty term) are included.

Table A.1: Sensitivity of the Regional Model to the Signal-to-Noise Penalty Weight.

	(i)	(ii)	(iii)	(iv)	(v)	(vi)
λ_{snr}	0e+00	1e+02	1e+04	1e+06	1e+08	1e+10
λ_{ekc}	1e+06	1e+06	1e+06	1e+06	1e+06	1e+06
γ	16.868	36.905	26.974	5.072	5.402	3.682
c_1	1.592	1.703	2.607	0.699	0.584	1.043
c_2	7.576	8.937	6.083	4.935	4.894	4.815
c_2^{Eur}	5.576	6.937	4.083	4.492	4.477	4.318
$\log(\sigma^2_\epsilon)$	-20.000	-20.000	-9.978	-7.030	-6.660	-6.597
$\log(\sigma^2_\eta)$	-6.706	-6.706	-6.811	-7.874	-8.041	-7.985
q-ratio	770.558	770.383	4.870	0.656	0.501	0.500
Log-likelihood	1131.36	1131.37	1130.08	1013.87	969.24	966.26
Log-likelihood (pen.)	1131.36	1131.25	1121.21	992.39	968.98	966.26

These results make the identification problem explicit. When the penalty is absent or negligible ($\lambda_{snr} = 0$ or 10^2), then the estimation degenerates: the observation noise σ_ε collapses towards its lower bound, the stochastic trend absorbs essentially all of the variation in the data ($q \approx 770$), the amplitude γ inflates to economically implausible values and the European shift is driven to its boundary ($c_2 - c_2^{Eur} = 2.0$, the imposed limit), as the DoS attempts to compensate. In these columns the non-penalized log-likelihood is high because a near-unrestricted random walk can track almost any smooth signal, but the resulting decomposition is not identified. The structural EKC cannot be longer separated from the trend.

As far as λ_{snr} is concerned, when it increases, the estimates stabilize. For $\lambda_{snr} \geq 10^6$ the signal-to-noise ratio settles close to the imposed threshold ($q \approx 0.5$–0.66), the amplitude stabilizes around $\gamma \approx 5$, the European early-mover gap settles at an economically sensible $c_2 - c_2^{Eur} \approx 0.42$–$0.44$, and the activation parameters c_1 and c_2 take sensible values. At the upper end of the grid the restriction ceases to be a soft constraint and imposes the ratio irrespective of the sample information. At $\lambda_{snr} = 10^{10}$ the ratio is pinned at $q = 0.500$ and the non-penalized log-likelihood falls to 966. The identified region is thus an interior one, flanked by degeneracy at both extremes.

Thus, the signal-to-noise penalty does not drive the estimates of the EKC and the European early-mover distance. It merely selects the identified solution from a region in which the log-likelihood function cannot distinguish the structural EKC curve from the trend. Moving from the unrestricted to the identified solution sacrifices some non-penalized log-likelihood value (roughly from 1131 to 1014), which is the cost of imposing an economically interpretable, gradual technological trend rather than an unrestricted one.

The second penalty, i.e. λ_{ekc}, does not play an role at the optimum of the log-likelihood function. Table A.2 shows that holding fixed $\lambda_{snr} = 10^6$ and varying λ_{ekc} over $\{0, 10^3, 10^6\}$ leaves every estimate numerically identical: the estimated amplitude ($\gamma \approx 5$) lies well above the threshold $\gamma \geq 1$, so the amplitude penalty is inactive and its weight is irrelevant to the reported solution. Identification is thus driven entirely by the signal-to-noise restriction. Thus, the second penalty is just a safeguard against degeneracy that does not materialize in our final specification.

Table A.2: Sensitivity of the Regional Model to the Amplitude Penalty Weight.

	(i)	(ii)	(iii)
λ_{snr}	1e+06	1e+06	1e+06
λ_{ekc}	0e+00	1e+03	1e+06
γ	5.072	5.072	5.072
c_1	0.699	0.699	0.699
c_2	4.935	4.935	4.935
c_2^{Eur}	4.492	4.492	4.492
$\log(\sigma_\epsilon^2)$	-7.030	-7.030	-7.030
$\log(\sigma_\eta^2)$	-7.874	-7.874	-7.874
q-ratio	0.656	0.656	0.656
Log-likelihood	1013.87	1013.87	1013.87
Log-likelihood (pen.)	992.39	992.39	992.39

Although the need of a discussion/proposal of a mainly data-driven selection criteria could come to the mind of some readers, it must be stated (based on the aforementioned findings) that there is no need for this and that it is enough to perform a sensitivity analysis as the one already presented above.

A.3 Bootstrap-based inference details

In this subsection further details on the bootstrap-based procedure used to conduct inference on the model parameters are provided.

Formal statistical inference for the DoS parameters $\{c_1, c_2, s_1, s_2, \gamma\}$ and the regional parameter c_2^{Eur} is necessary to assess the statistical significance of the structural coefficients. In particular, it allows to determine whether the difference $c_2 - c_1 > 0$, which is required for the EKC interpretation, and the difference $c_2 - c_2^{\mathrm{Eur}} > 0$, associated with the European early-mover result, are statistically significant. It also provides whether the amplitude γ is distinguishable from zero. Standard errors, confidence intervals and test statistics are therefore computed for the parameters of the panel regression model with stochastic trends. This information also makes it possible to assess the statistical significance of coefficients and distances between coefficients and to construct a confidence interval around the EKC function.

Table 2 of the main paper reports standard errors for the structural parameters. These are obtained based on the seminal paper for bootstrap-based inference for State-Space models developed by Stoffer and Wall (1991), which is based on the prediction errors from the Kalman filter and is adapted here to the new framework we propose. The procedure is as follows:

1. We set the parameter vector ψ equal to its (penalized) maximum likelihood estimate $\widehat{\psi}$, apply the Kalman filter to the data where the fixed effects and the difference-of-sigmoids (EKC) curve are subtracted, that is, $z_{it} = y_{it} - \hat{\mu}_i - \hat{\gamma} EKC(\widehat{\psi})$, and collect the prediction errors $v_{it} = z_{it} - \mathrm{E}(z_{it}|Z_{t-1}; \widehat{\psi})$ for $i = 1, \dots, N$ and $t = 2, \dots, T$, where $Z_s = \{z_{12}, \dots, z_{N2}, z_{13}, \dots, z_{N,s}\}$ with $2 \le s \le T$, by applying the Kalman filter. We notice that we discard the errors at time $t = 1$ because they are ill-defined in the Kalman filter.

2. In a correctly specified model, the prediction errors are mutually (across i) and serially (across t) independent of each other. Serial correlation in the model is specified with some flexibility (stochastic trends) and empirical evidence is presented that the remaining serial correlation in the errors is negligible. However, the cross-sectional dimension in the model is more restrictively specified by the EKC with pooled coefficients. We therefore are left with prediction errors that exhibit strong cross-sectional dependence, see Figure 9 in the revised paper. We correct for this dependence by pre-whitening $v_t = (v_{1t}, \dots, v_{Nt})'$, for $t = 2, \dots, T$, using the symmetric root of their empirical variance matrix

$$\widetilde{\Sigma} = \frac{1}{T-1} \sum_{t=2}^{T} v_t \, v_t',$$

   and by computing $u_t = \widetilde{\Sigma}^{-1/2} v_t$, for $t = 2, \dots, T$, which have a unity variance matrix as is appropriate for the bootstrap method.

3. The pre-whitened prediction errors are resampled with replacement from all elements in the $N \times (T-1)$ matrix $[u_2, \dots, u_T]$, as dictated by the Stoffer-Wall bootstrap procedure, to obtain a set of B samples of series of bootstrap-based synthetic prediction errors, denoted by $u_t^{(b)} = (u_{1t}^{(b)}, \dots, u_{Nt}^{(b)})'$, for $b = 1, \dots, B$. To re-instate the corresponding bootstrap resample for the v_t's, we compute $v_t^{(b)} = \widetilde{\Sigma}^{1/2} u_t^{(b)}$. The Stoffer-Wall inverse-Kalman filter (or innovation form) is adopted to obtain the bootstrap-based synthetic panel $Z_T^{(b)}$, for $b = 1, \dots, B$. Finally, fixed effects and the EKC are added to each element $z_{it}^{(b)}$ and bootstrap replicates of the panel data set in the observation space are obtained.

4. Based on each bootstrap-based synthetic panel data set, the *entire* parameter vector (including the nonlinear DoS parameters) is re-estimated using the same penalized log-likelihood function and the same optimizer. In this way, we obtain a set of B bootstrapped estimates of ψ from which standard errors and percentile-based confidence intervals of the elements in $\widehat{\psi}$ can be constructed.

B Further empirical insights

B.1 Linear deterministic trends as a possible alternative to the methodological proposals of the main paper.

It is of interest to augment the model proposed in subsection in 4.3 of the main paper to be able to include country-specific linear deterministic trends, t_i. Then, the comparison to both models included in 4.3 as well as to the stochastic model in 4.4 are provided.

The static panel model (2.1) have been extended for its treatment in Section 4.3 by having country-specific linear deterministic trends, giving the following model:

$$y_{it} = \mu_i + \delta_i\, t + \gamma\,[\sigma_1(x_{it}) - \sigma_2(x_{it})] + \varepsilon_{it},$$

The same estimation method as in Section 4.3 is used (also with the same starting values, parameter bounds and optimizer).

The three model specifications compared in Table B.3 share the same global difference-of-sigmoids (DoS) curve and differ only in how the country baseline is modeled. For the two static specifications, the log-likelihood reported is the concentrated Gaussian log-likelihood implied by the residual sum of squares over all $15 \times 40 = 600$ observations. The two models are nested, and the likelihood ratio statistic of the augmented specification against the fixed-effects model is 653.6 on 15 degrees of freedom. The figure provided for the stochastic-trend model is the penalized objective reported in Table 2 of the main paper, but it is not directly comparable, since it is evaluated by the Kalman filter after the diffuse initialization (thus, on a smaller effective sample and it includes the identifying penalty).

Table B.3: Estimated Structural Parameters under Alternative Treatments of the Country Baseline.

	Fixed effects	+ Linear trends	+ Stochastic trends
γ	37.534	16.620	3.715
c_1	3.239	2.070	1.106
c_2	3.968	2.074	4.564
s_1	0.612	0.189	1.040
s_2	0.636	$0.000^{\dagger}$	4.501
Log-likelihood	523.25	850.04	984.83

Note: †Estimate at the lower bound of the parameter space, so that the second logistic reduces to a constant and the curve becomes monotonically increasing, with no emissions peak.

The inclusion of the linear trends in the model leads to a collapse of the EKC. The two activation thresholds are estimated close to each other ($c_1 = 2.070$ and $c_2 = 2.074$, a separation of 0.004 against 3.458 in the dynamic model), and the green-transition slope is estimated close to the lower bound of the parameter space ($\widehat{s}_2 = 10^{-6}$), where s_2 at zero let the second logistic in the DoS become a constant. Hence, the DoS function reduces to an increasing curve with no peak. The same two problems are reported in Section 4.2 when we reject individual, country-by-country, estimates: thresholds that coincide, which contradicts the 'grow first, clean later' interpretation, and a slope coefficient that often degenerates to its numerical bound.

Further insights can be provided by presenting the estimated trend slopes in Table B.4, in log-points of CO_2 per capita, per year. The estimated slopes are negative for every advanced economy, the United Kingdom (-0.026), Germany (-0.027), France (-0.023) and the United States (-0.017), and positive for most emerging countries. The linear trends therefore take over the fall in emissions of the developed countries, which is exactly what the descending part of the DoS is meant to capture. Once the trends absorb it, there is nothing left for the second logistic to explain, and it switches off.

Table B.4: Estimated Country-Specific Deterministic Trend Slopes.

Argentina	Australia	Brazil	Canada	China
-0.0059	-0.0112	+0.0020	-0.0135	+0.0028
France	Germany	India	Indonesia	Italy
-0.0226	-0.0266	+0.0076	+0.0059	-0.0129
Japan	Mexico	Turkey	United Kingdom	United States
-0.0044	-0.0111	-0.0002	-0.0263	-0.0170

Table B.5 reports the residual diagnostics computed equation by equation across the 15 countries. ADF rejections count the countries for which the unit root null is rejected at the 5% level, and Ljung-Box non-rejections those for which the white-noise null is not rejected at the same level. Higher counts are better in both cases.

Table B.5: Residual Diagnostics under Alternative Treatments of the Country-Level Baseline.

	Fixed effects	+ Linear trends	+ Stochastic trends
ADF rejections	0/15	0/15	12/15
Ljung–Box non-rejections	0/15	0/15	13/15

The inclusion of linear trends delivers better residuals: the average of first-order residual autocorrelation falls from 0.84 to 0.75. However, the linear trends do not solve the problem that motivates the development in Section 4.4: the inclusion of stochastic trends. As for the model with fixed effects only treated in Section 4.3, neither the null of unit-root nor the null of white-noise is rejected for any of the fifteen countries. Linear trends just cannot absorb the changing shapes of the energy transitions in the individual countries, while the stochastic trends can, see Figure 8 in the main paper. This comparison is also relevant for dealing with possible concerns of overfitting related to Figure 8 in the main paper. Most extracted trends are far from resembling straight lines, even when imposing the same signal-to-noise ratio. This clearly indicates that the extra structure in $\widehat{\tau}_{it}$ is genuine. For example, the stochastic trends feature the long non-linear decline in France after the Messmer plan (the large-scale civil nuclear-power program announced in March 1974), the break after 1990 in the United Kingdom or the restructuring of the former East Germany. These examples emphasize that the stochastic trend describes a signal rather than noise. Also, without the inclusion of stochastic trends, we have given evidence that residuals are $I(1)$, see Table B.5.

B.2 Discussion of the non-stationarity of the data and the DoS transformation

Given that a central motivation for the state-space extension is to address the critique of Wagner (2015), according to which applying nonlinear transformations of integrated regressors in a cointegrating regression framework can produce spurious results. The stochastic trend component of our proposal is designed to capture the non-stationarity that the DoS transformation cannot accommodate. Thus, the integration properties of both the raw series and the DoS-transformed regressor can be established formally.

In this Section, results on the underlying data being $I(1)$ using standard panel unit root tests allow confirming that the DoS-transformed variable $\sigma_j(x_{it}; c_j, s_j)$ is bounded in $[0, 1]$ and is therefore stationary, $I(0)$, and this holds even when x_{it} is $I(1)$. This boundedness property is precisely the feature that distinguishes the DoS specification introduced in this paper from the polynomial EKC, where powers of an $I(1)$ process yield unbounded, fractionally integrated or non-integrated processes.

To clarify why the proposed model remains immune to the polynomial cointegration critique, empirical evidence on the order of integration of the two underlying series is included in Table B.6, where the augmented Dickey-Fuller (ADF) tests are reported for $\ln \text{GDP}_{it}$ and $\ln \text{CO}_{2it}$ for each country, together with the Engle-Granger cointegration test.

Table B.7 shows the corresponding panel versions of the test statistics. Since the panel exhibits strong cross-sectional dependence, we adopt the second-generation CIPS test proposed by Pesaran (2007), which is robust to this dependence in contrast to the first-generation LLC and IPS tests (see discussion in Pesaran paper). The CIPS test is computed in levels and in differences. It can be stated from these results that the time series are integrated of order 1 with strong support for all countries.

Table B.6: Univariate Integration and Cointegration Tests.

Country	GDP Level	GDP Diff.	CO_2 Level	CO_2 Diff.	EG Stat.	EG (p-val)
Argentina	0.2830	$\leq$0.01**	0.3100	$\leq$0.01**	-2.174	$\geq$0.10
Brazil	0.3470	$\leq$0.01**	0.2310	$\leq$0.01**	-2.621	0.0979
China	0.9430	0.014**	0.8880	$\leq$0.01**	-3.182	0.0353**
India	0.9800	$\leq$0.01**	0.6110	$\leq$0.01**	-1.497	$\geq$0.10
Indonesia	0.5690	$\leq$0.01**	0.2000	$\leq$0.01**	-1.921	$\geq$0.10
Mexico	0.3790	$\leq$0.01**	0.6280	$\leq$0.01**	-1.204	$\geq$0.10
Turkey	0.0600	$\leq$0.01**	0.6880	$\leq$0.01**	-1.289	$\geq$0.10
Australia	0.9810	$\leq$0.01**	0.9900	$\leq$0.01**	-1.670	$\geq$0.10
Canada	0.8010	$\leq$0.01**	0.7140	$\leq$0.01**	-1.210	$\geq$0.10
France	0.9530	$\leq$0.01**	0.3360	$\leq$0.01**	-1.414	$\geq$0.10
Germany	0.1780	$\leq$0.01**	0.1940	$\leq$0.01**	-2.066	$\geq$0.10
Italy	0.9890	$\leq$0.01**	0.9900	$\leq$0.01**	-0.801	$\geq$0.10
Japan	0.5910	$\leq$0.01**	0.9750	$\leq$0.01**	-0.887	$\geq$0.10
United Kingdom	0.9460	0.016**	0.9900	$\leq$0.01**	-1.204	$\geq$0.10
United States	0.9300	$\leq$0.01**	0.9780	$\leq$0.01**	-1.176	$\geq$0.10

Note: ADF tests (H_0: unit root) use drift and trend in levels, drift only in differences. Engle-Granger (EG) tests H_0: no cointegration. Asterisks (**) denote rejection of the null at the 5% significance level. The p-values are reported where the tabulated critical values resolve, and as bounds ($\leq$0.01, $\geq$0.10) otherwise.

Table B.7: Panel Cross-Sectional Dependence and Unit-Root Tests.

	GDP		CO_2	
Test	Stat.	p-val	Stat.	p-val
CIPS (levels)	-2.165	$\geq$0.10	-1.791	$\geq$0.10
CIPS (differences)	-3.311	$\leq$0.01**	-4.237	$\leq$0.01**
LLC (levels)	-1.569	0.0583	2.060	0.9803
IPS (levels)	0.031	0.5123	1.307	0.9043

Note: CIPS, LLC and IPS tests for H_0: unit root, are discussed in Pesaran (2007). The CIPS test is robust to cross-sectional dependence, the LLC and IPS tests are not. Levels include drift and trend, differences include drift only. LLC reports the z statistic, IPS the W_{tbar} statistic, so the two are not comparable in magnitude. Asterisks (**) denote rejection of the null at the 5% significance level.

References

Apergis, N. and J. E. Payne (2009). CO_2 emissions, energy usage, and output in Central America. *Energy Policy 37*, 3282–86.

Bennedsen, M., E. Hillebrand, and S. Jensen (2023). A neural network approach to the environmental Kuznets curve. *Energy Economics 126*, 106985.

Bennedsen, M., E. Hillebrand, and S. J. Koopman (2023). A multivariate dynamic statistical model of the global carbon budget 1959-2020. *Journal of the Royal Statistical Society, Series A 186*, 20–42.

Bolton, P. and M. Kacperczyk (2021). Do investors care about carbon risk? *Journal of Financial Economics 142*, 517–49.

Byrd, R. H., P. Lu, J. Nocedal, and C. Zhu (1995). A limited memory algorithm for bound constrained optimization. *SIAM Journal on Scientific Computing 16*, 1190–208.

Castle, J. L. and D. F. Hendry (2026). The 'Climate Kuznets Curve': A Critique. *Energy Economics 157*, 109231.

Cole, M. A., A. J. Rayner, and J. M. Bates (1997). The EKC: an empirical analysis. *Environment and Development Economics 2*, 401–16.

De Jong, R. M. and M. Wagner (2025). Panel cointegrating polynomial regression analysis and an illustration with the environmental Kuznets curve. *Econometrics and Statistics 33*, 135–65.

Dell, M., B. F. Jones, and B. A. Olken (2012). Temperature shocks and economic growth: evidence from the last half century. *American Economic Journal: Macroeconomics 4*, 66–95.

Durbin, J. and S. J. Koopman (2012). *Time Series Analysis by State Space Methods* (2nd ed.). Oxford: Oxford University Press.

Fosten, J., B. Morley, and T. Taylor (2012). Dynamic misspecification in the EKC. *Energy Policy 45*, 364–73.

Friedlingstein, P., M. O'Sullivan, M. W. Jones, et al. (2025). Global Carbon Budget 2025. *Earth System Science Data 17*, 1–50.

Gao, J. and K. Hawthorne (2006). Semiparametric estimation and testing of the trend of temperature series. *Econometrics Journal 9*, 332–55.

Grossman, G. M. and A. B. Krueger (1991). Environmental impacts of a North American Free Trade Agreement. Working Paper 3914, National Bureau of Economic Research, Cambridge, MA.

Grossman, G. M. and A. B. Krueger (1995). Economic growth and the environment. *Quarterly Journal of Economics 110*, 353–77.

Hansen, B. E. (1999). Threshold effects in non-dynamic panels. *Journal of Econometrics 93*, 345–68.

Harvey, A. C. (1989). *Forecasting, Structural Time Series Models and the Kalman Filter.* Cambridge: Cambridge University Press.

Holtz-Eakin, D. and T. M. Selden (1995). Stoking the fires? CO_2 emissions and economic growth. *Journal of Public Economics 57*, 85–101.

IPCC (2023). Climate change 2023: Synthesis report. Technical report, Intergovernmental Panel on Climate Change, Geneva.

Keane, M. and T. Neal (2020). Comparing deep neural network and econometric approaches to predicting the impact of climate change on agricultural yield. *Econometrics Journal 23*, S59–S80.

Koopman, S. J., N. Shephard, and J. A. Doornik (1999). Statistical algorithms for models in state space using SsfPack 2.2. *Econometrics Journal 2*, 107–60.

Kuznets, S. (1955). Economic growth and income inequality. *American Economic Review 45*, 1–28.

Leal, P. H. and A. C. Marques (2022). The evolution of the environmental Kuznets curve hypothesis assessment: a literature review under a critical analysis perspective. *Heliyon 8*, e11521.

Li, R., Q. Wang, and J. Guo (2024). Revisiting the environmental Kuznets curve (EKC) hypothesis of carbon emissions: exploring the impact of geopolitical risks, natural resource rents, corrupt governance, and energy intensity. *Journal of Environmental Management 351*, 119663.

List, J. A. and C. A. Gallet (1999). The environmental Kuznets curve: does one size fit all? *Ecological Economics 31*, 409–23.

Maddison, D. (2006). Environmental Kuznets curves: a spatial econometric approach. *Journal of Environmental Economics and Management 51*, 218–30.

Montagna, S., L. Huang, Y. Long, and Y. Yoshida (2025). Sectoral economic complexity and environmental degradation: a sectoral perspective on the EKC hypothesis. *Nature: Humanities and Social Sciences Communications 12*, 764.

OECD (2017). *Investing in Climate, Investing in Growth.* Paris: OECD Publishing.

Panayotou, T. (1993). Empirical tests and policy analysis of environmental degradation at different stages of economic development. Working Paper 238, International Labour Organization, Geneva.

Peña, D. and G. E. P. Box (1987). Identifying a simplifying structure in time series. *Journal of the American Statistical Association 82*, 836–43.

Perman, R. and D. I. Stern (2003). Evidence from panel unit root and cointegration tests that the environmental Kuznets curve does not exist. *Australian Journal of Agricultural and Resource Economics 47*, 325–47.

Pesaran, M. H. (2007). A simple panel unit root test in the presence of cross-section dependence. *Journal of Applied Econometrics 22*, 265–312.

Phillips, P. (1987). Time series regression with a unit root. *Econometrica 55*, 277–301.

Roser, M., H. Ritchie, E. Ortiz-Ospina, and J. Hasell (2024). Our World in Data. https://ourworldindata.org.

Shafik, N. and S. Bandyopadhyay (1992). Economic growth and environmental quality: time-series and cross-country evidence. Policy Research Working Paper 904, World Bank, Washington, DC.

Stern, D. I. (2004). The rise and fall of the environmental Kuznets curve. *World Development 32*, 1419–39.

Stoffer, D. S. and K. D. Wall (1991). Bootstrapping state-space models: Gaussian maximum likelihood estimation and the Kalman filter. *Journal of the American Statistical Association 86*, 1024–1030.

UNFCCC (1997). Kyoto protocol to the united nations framework convention on climate change.

UNFCCC (2015). Paris agreement.

Wagner, M. (2015). The environmental Kuznets curve, cointegration and nonlinearity. *Journal of Applied Econometrics 30*, 948–67.

Wagner, M., P. Grabarczyk, and S. H. Hong (2020). Fully modified OLS estimation and inference for seemingly unrelated cointegrating polynomial regressions and the environmental Kuznets curve for carbon dioxide emissions. *Journal of Econometrics 214*, 216–55.

Wang, Q., Y. Li, and R. Li (2024). Rethinking the environmental Kuznets curve hypothesis across 214 countries: the impacts of 12 economic, institutional, technological, resource, and social factors. *Nature: Humanities and Social Sciences Communications 11*, 292.

Wang, Q., X. Wang, R. Li, and X. Jiang (2024). Reinvestigating the environmental Kuznets curve (EKC) of carbon emissions and ecological footprint in 147 countries: a matter of trade protectionism. *Nature: Humanities and Social Sciences Communications 11*, 160.

World Bank (2024). World Development Indicators.